The Photochemical Generation of Hydroxyl Radicals in the UV-vis/ Ferrioxalate/H2O2 System

ARTICLE *in* ENVIRONMENTAL SCIENCE & TECHNOLOGY · SEPTEMBER 1999

Impact Factor: 5.33 · DOI: 10.1021/es9810134

2 AUTHORS, INCLUDING:

James R Bolton
University of Alberta
315 PUBLICATIONS **9,533** CITATIONS

Environ. Sci. Technol. **1999**, *33,* 3119−3126

The Photochemical Generation of Hydroxyl Radicals in the UV−vis/Ferrioxalate/H_2O_2 System

KELLY A. HISLOP AND JAMES R. BOLTON*

Photochemistry Unit, Department of Chemistry, The University of Western Ontario, London, Ontario, Canada N6A 5B7

A reaction mechanism has been validated for the photochemical generation of hydroxyl radicals by ultraviolet or visible irradiation of oxalato iron(III) complexes (ferrioxalate) in the presence of hydrogen peroxide and 2-propanol as a model substrate. A kinetic simulation program incorporating the set of reactions was written to predict the behavior of this photochemical system. The program calculates the quantum yield of oxidation of 2-propanol used as a hydroxyl radical scavenger. The scavenger's oxidation product, 2-propanone, was analyzed by gas chromatography after controlled exposure of the solution to a calibrated light source. The theoretical quantum yields of 2-propanol oxidation, Φ_{RH}, agreed reasonably well with experimentally determined Φ_{RH} values under a variety of initial reaction conditions. The value of Φ_{RH}, which under appropriate conditions is directly proportional to the quantum yield for the generation of hydroxyl radicals, Φ_{OH}, was considerably greater than unity in most cases (often $\Phi_{RH} = 3.0-4.0$), indicative of a chain mechanism involving iron cycling between the II and III oxidation states.

Introduction

Much is known concerning the nature of the Fenton reaction, first described in a paper that appeared in 1894 (*1*). In recent decades, attention has turned to its possible application in oxidative treatments of contaminated water because it produces the hydroxyl radical •OH, a powerful oxidizer capable of degrading many organic compounds (*2*), in a spontaneous dark reaction:

$$Fe^{2+} + H_2O_2 \rightarrow Fe^{3+} + {}^{\bullet}OH + OH^- \quad (1)$$

A variation of reaction 1, called the photo-Fenton reaction, combines ultraviolet (and some visible) light, Fe(III), and hydrogen peroxide. It can also facilitate the production of hydroxyl radicals by a photochemical route (*3*−*5*)

$$Fe(OH)^{2+} + h\nu \rightarrow Fe^{2+} + {}^{\bullet}OH \quad (2)$$

followed by reaction 1. More importantly, iron is cycled between the +2 and +3 oxidation states, so Fe(II) is not depleted, and •OH production is limited only by the availability of light and H_2O_2. $Fe(OH)^{2+}$, the dominant iron(III)−hydroxy complex in mildly acidic solutions (pH 2.5−5) photolyses in the UV−vis range (to ∼400 nm) but with a relatively low quantum yield (e.g., $\Phi_{Fe(II)} = 0.14 \pm 0.04$ at 313 nm (*3*); $\Phi_{OH} = 0.195 \pm 0.033$ at 310 nm (*6*)).

The quantum yield of Fe(II) production, $\Phi_{Fe(II)}$, greatly increases when Fe(III) is complexed with a carboxylic anion, such as oxalate (e.g., $\Phi_{Fe(II)} = 1.24$ at 300 nm, pH ∼2, and 6 mM ferrioxalate (*7*)). The ferrioxalate complex $[Fe(C_2O_4)_3]^{3-}$ is highly photosensitive and is used as the basis of a well-known chemical actinometer (*8*). The reduction of Fe(III) to Fe(II), through a photoinduced ligand to metal charge transfer, can occur over the ultraviolet and into the visible (out to ∼550 nm) (*9*):

$$Fe^{III}(C_2O_4)_3^{3-} \xrightarrow{h\nu} Fe^{2+} + 2C_2O_4^{2-} + C_2O_4^{\bullet-} \quad (\Phi_{Fe(II)}N_a/V) \quad (3)$$

$$C_2O_4^{\bullet-} \xrightarrow{k_4} CO_2^{\bullet-} + CO_2 \quad (4)$$

$$CO_2^{\bullet-} + Fe^{III}(C_2O_4)_3^{3-} \xrightarrow{k_5} Fe^{2+} + CO_2 + 3C_2O_4^{2-} \quad (5)$$

The overall rate of Fe(II) formed by reactions 3−5 is $\Phi_{Fe(II)}N_a/V$ ($M\,s^{-1}$), where $\Phi_{Fe(II)}$ is the quantum yield of iron(II) generation, N_a is the absorbed photon flux (einstein s^{-1}), and V is the volume (L) irradiated. One einstein is equal to one mole of photons. While the quantum yield of the primary photochemical step (reaction 3) is less than unity, the net value of $\Phi_{Fe(II)}$ can be greater than one as a result of formation of the oxalyl radical anion $C_2O_4^{\bullet-}$, which quickly decomposes to the carbon dioxide radical anion $CO_2^{\bullet-}$[$k_4 = 2 \times 10^6$ s^{-1} (*10*)]. This reducing agent can produce Fe(II) via reaction 5 (*11*,*12*).

When ferrioxalate is irradiated in the presence of H_2O_2, the Fenton reaction occurs to produce, under ideal conditions, one •OH for every Fe(II) generated (*13*). Here, Fe^{2+}

$$Fe^{2+} + H_2O_2 + 3C_2O_4^{2-} \xrightarrow{k_6} Fe^{III}(C_2O_4)_3^{3-} + OH^- + {}^{\bullet}OH \quad (6)$$

represents the sum of uncoordinated Fe(II) and $[Fe^{II}C_2O_4]^0$, both of which are able to react with H_2O_2. Therefore, k_6 is the apparent second-order rate constant for the reaction between Fe^{2+} and H_2O_2. In the presence of a sufficient excess of oxalate, Fe(III) will coordinate with either two or three oxalate ligands. As with the photo-Fenton reaction, iron cycles between oxidation states and so the production of hydroxyl radicals is limited only by the availability of light, H_2O_2, and oxalate, the latter two of which are depleted during the reaction.

The combination of ultraviolet and/or visible light (out to 550 nm), ferrioxalate as the primary absorber, and H_2O_2 has recently been patented for use in the wastewater treatment industry as an Advanced Oxidation Technology (AOTs) (*14*,*15*). While the oxidation of a number of organic compounds using this method has been demonstrated using both artificial and solar irradiation (*16*−*20*), detailed mechanistic studies of systems containing Fe(III) coordinated with oxalate have been generally limited to the very low reactant concentrations typical of natural surface and atmospheric waters (*21*−*24*). Here, the relative reactant concentrations are very different from those used in this investigation and so the reaction mechanism could differ.

Ferrioxalate has been used to reduce compounds that are resistant to oxidation. Huston and Pignatello (*25*) sensitized the removal of halogen atoms from perchloroalkanes using carbon dioxide radical anions $CO_2^{\bullet-}$ generated from irradiated ferrioxalate (in the absence of H_2O_2). The reduction products of the perchloroalkanes, stable under

* Corresponding author; phone: (519) 661-2170; fax: (519) 661-3022; e-mail: jbolton@julian.uwo.ca.

10.1021/es9810134 CCC: $18.00
Published on Web 07/31/1999

these conditions, were then oxidized by simply adding H_2O_2 to generate •OH radicals via reaction 6.

In the present study, absolute quantum yields of substrate oxidation, Φ_{RH}, not previously reported for this system, were determined for different initial reaction conditions. The reaction mechanism for the UV−vis/ferrioxalate/H_2O_2 system in the presence of 2-propanol, an oxidizable organic substrate, was then validated by comparing the experimental results with theoretical quantum yields, generated by a kinetic simulation program modeled on the reaction mechanism. Relatively high substrate concentrations were used for most experiments, such that the substrate was the sole scavenger of •OH. Under such conditions, Φ_{RH} is an indirect measure of the quantum yield of •OH generation, Φ_{OH}.

Very short exposure times were used in the irradiation of reaction mixtures, such that the percent conversion of 2-propanol to its principal oxidation product, 2-propanone (*26*), was below 1%. Therefore, there were no significant interferences from the primary oxidation products, and no secondary oxidation products were formed. Furthermore, 2-propanone has a lower rate constant ($1.1 \times 10^8\ M^{-1}\ s^{-1}$ (*2*)) for reaction with •OH than does 2-propanol ($1.9 \times 10^9\ M^{-1}\ s^{-1}$ (*2*)).

The efficiency with which •OH is produced, as inferred in this study from the value Φ_{RH}, is important with respect to its application as an AOT. High efficiencies may translate to lower radiative energy requirements, and energy can be a large contributor to the operating cost of an AOT. Therefore, an understanding of the reaction mechanism, and thereby how the quantum yield can be optimized, is of particular interest.

Materials and Methods

Reagents. As a result of its light sensitivity, ferrioxalate was prepared under a red photographic "safe" light immediately prior to the time of use. It was prepared from a ferric sulfate (J. T. Baker Chem. Co., Phillipsberg, NJ, reagent grade) solution in dilute H_2SO_4 and a potassium oxalate (British Drug Houses (BDH), Poole, England, reagent grade) solution in a 1:3.2 molar ratio. Oxalate was added in excess to ensure that virtually all of the Fe(III) would be complexed with either two or three oxalate anions, with a significant fraction as the trioxalato complex [see (*21*) for formation constants]. Distilled, deionized water was used for all solutions. Ferric sulfate was standardized spectrophotometrically by complexing reduced iron with 1,10-phenanthroline in a sodium acetate buffer (pH 4) and measuring its absorbance at 510 nm. Reagent-grade 2-propanol (Fisher Scientific Co., Fair Lawn, NJ) and 30% H_2O_2 stock solutions (BDH) were used as received. The ferrioxalate stock solution was acidic, so the final pH of the reaction mixtures was 2.2 ± 0.1, unless otherwise stated. For experiments in which the concentration of ferrioxalate was varied, pH adjustment of reaction mixtures to a constant value was necessary prior to irradiation. A concentrated sodium hydroxide (BDH) solution (10 M) was used for this purpose.

Apparatus and Irradiation Procedures. A Photon Technologies International Quantacount Apparatus was used to expose reaction mixtures (contained in a 1.000-cm quartz cuvette) to a known number of photons at a chosen wavelength with magnetic stirring via a cell stirring bar. All mixtures were at room temperature (22−27 °C). An Osram HBO 100 W short arc mercury lamp was used as the light source. A monochromator, with variable entrance and exit slits and a shutter assembly, allowed controlled light exposure at the selected wavelength. The photon flux of the lamp was determined using ferrioxalate actinometry (*7*).

After controlled light exposure of the ferrioxalate/H_2O_2/2-propanol solutions was complete, 10 M NaOH was added to precipitate the iron as iron oxyhydroxide and prevent further production of •OH. The precipitate was subsequently removed by filtration through a plug of glass wool.

Analysis of 2-Propanone and Quantum Yield Determinations. Because of the low percent conversion of 2-propanol to 2-propanone, the number of moles of 2-propanone generated was measured. This is more accurate than the measurement of very small changes in the concentration of 2-propanol, which was present in excess.

Oxidation of 2-propanol by •OH occurs by abstraction of the OH group hydrogen atom (1.2%) to form an oxyl radical or of a carbon bound hydrogen to form the α- and β-hydrogen abstracted radicals (85.5 and 13.3% respectively) (*27*). However, only the oxyl and α-radicals lead to the formation of 2-propanone. Therefore, •OH attack of 2-propanol gives an 86.7% yield of 2-propanone. Furthermore, the oxidation of these organo radicals to 2-propanone is achieved by reaction with either oxygen or Fe(III) and so the yield of 2-propanone should be independent of oxygen concentration in the presence of Fe(III) (*6*). Hence, the amount of 2-propanone generated can be used, as shown in eq 7, to determine the experimental quantum yield of 2-propanol oxidation, Φ_{RH}:

$$\Phi_{RH} = \frac{\text{moles 2 − propanone}}{\text{einsteins light absorbed}} \times \frac{1}{0.867} \qquad (7)$$

The concentration of 2-propanone generated was analyzed using a Perkin-Elmer Sigma 2B Gas Chromatograph and a Hewlett-Packard 3396 Series II Integrator. The pH of each of the filtered aqueous samples was lowered to a suitable range (~6.5−8.0) before injection to prevent damage to the analytical column stationary phase. Samples were manually injected (in 1-μL volumes) into a heated (200 °C) flash vaporization injector. A DB-624 column (30 m × 0.53 mm, Chromatographic Specialties) eluted 2-propanone at 1.9 min and 2-propanol at 2.2 min (Helium carrier gas linear flow rate of 82 cm s^{-1}; column temperature, 32 °C). The flame ionization detector temperature was 220 °C. For each sample, and immediately after the elution of 2-propanol, the column was heated to 85 °C to remove condensed water.

Additional Methods: For experiments that investigated the effect of oxygen on Φ_{RH}, reaction mixtures were sparged with compressed gases of varying oxygen/nitrogen composition for at least one-half hour immediately prior to irradiation. The oxygen concentration was measured using an Orion Dissolved Oxygen Meter (model 840) which displays the concentration in mg of oxygen L^{-1}. For all other experiments, the initial oxygen concentration was assumed to be that in air-equilibrated water (0.27 mM).

Hydrogen peroxide concentrations were determined using the triiodide method described by Klassen et al. (*28*). To determine formaldehyde (formed when methanol was used in the place of 2-propanol as an •OH scavenger), exposed reaction mixtures were first taken to neutral pH and the H_2O_2 destroyed using bovine catalase. A complex of formaldehyde and dinitrophenylhydrazine was prepared according to a method described by Wells (*29*). Iron precipitates were removed by filtration prior to measuring the solution absorbance at 420 nm.

Results and Discussion

Validation of the Φ_{RH} Method. The analytical methods and experimental approach were verified by determining a well-known quantum yield—that for the production of •OH from directly photolyzed H_2O_2. A concentration of 51.5 mM 2-propanol was used to scavenge essentially all (99.6%) •OH produced by photolyzing 12.7 mM H_2O_2 at 254 nm. This was above the experimentally observed minimum concentration (~10 mM) of 2-propanol required to scavenge virtually all •OH. Therefore, Φ_{RH} is equal to Φ_{OH}. A plot of moles of

TABLE 1. Main Reactions Used in the Simulation Program

reaction number	reaction	unknown values (used as adjustable parameters)
–	$Fe^{2+} + C_2O_4^{2-} \rightleftharpoons [Fe^{II}C_2O_4]^0$	$K_{FeOx} = 5.9 \times 10^3\ M^{-1}$
6	$Fe^{2+} + H_2O_2 + 3\ C_2O_4^{2-} \rightarrow Fe^{III}(C_2O_4)_3^{3-} + OH^- + {}^\bullet OH$	$(f_{Fe(II)}k_{Fe(II)} + f_{FeOx}k_{FeOx})\ M^{-1}\,s^{-1}$ [a]
11	${}^\bullet OH + HC_2O_4^- \rightarrow H_2O + C_2O_4^{\bullet -}$	$9.0 \times 10^7\ M^{-1}\,s^{-1}$
13	${}^\bullet ROH + Fe^{III}(C_2O_4)_3^{3-} \rightarrow RO + Fe^{2+} + 2\ C_2O_4^{2-} + HC_2O_4^-$	$7.5 \times 10^8\ M^{-1}\,s^{-1}$ [b]
17	$HO_2^\bullet + Fe^{III}(C_2O_4)_3^{3-} \rightarrow Fe^{2+} + H^+ + O_2 + 3\ C_2O_4^{2-}$	$3.5 \times 10^3\ M^{-1}\,s^{-1}$
		known values
8	$Fe^{III}(C_2O_4)_3^{3-} + h\nu \rightarrow Fe^{2+} + 2.5\ C_2O_4^{2-} + CO_2$	$\Phi_{Fe(II)}\ N_a/V\ (M\ s^{-1})$ [c]
9	${}^\bullet OH + HROH \rightarrow {}^\bullet ROH + H_2O$	$1.9 \times 10^9\ M^{-1}\,s^{-1}$ (*2*)
10	${}^\bullet OH + H_2O_2 \rightarrow H_2O + HO_2^\bullet$	$2.7 \times 10^7\ M^{-1}\,s^{-1}$ (*2*)
12	${}^\bullet OH + SO_4^{2-} + H^+ \rightarrow H_2O + SO_4^{\bullet -}$	$1.2 \times 10^6\ M^{-1}\,s^{-1}$ (*2*)
14	${}^\bullet ROH + O_2 \rightarrow RO + HO_2^\bullet$	$4.1 \times 10^9\ M^{-1}\,s^{-1}$ [d]
15	$Fe^{2+} + HO_2^\bullet + H^+ + 3\ C_2O_4^{2-} \rightarrow Fe^{III}(C_2O_4)_3^{3-} + H_2O_2$	$(1.2 \pm 0.2) \times 10^6\ M^{-1}\,s^{-1}$ [e]
16	$HO_2^\bullet + HO_2^\bullet \rightarrow H_2O_2 + O_2$	$(8.3 \pm 0.7) \times 10^5\ M^{-1}\,s^{-1}$ (*36*)

[a] The apparent rate constant k_6 was not used as an adjustable parameter, but its value is dependent on the adjustable parameter K_{FeOx}. The value of k_6 was calculated using the mole fractions f of Fe(II) and $[Fe^{II}C_2O_4]^0$, found using the formation constant K_{FeOx} for the complex of Fe(II) and the dibasic oxalate anion. [b] The rate constants reported in the literature for the reaction between ${}^\bullet ROH$ and *uncomplexed* Fe(III) are 5.8×10^8, 1.8×10^8, and $4.5 \times 10^8\ M^{-1}\,s^{-1}$ (*37*). [c] The experimental data were obtained using 300-nm light, where $\Phi_{Fe(II)} = 1.2$ (*7*). [d] This value is the average of three rate constants given in ref *37*. [e] The literature rate constant for the reaction between *uncomplexed* Fe(II) and the hydroperoxyl radical $(1.2 \pm 0.2) \times 10^6\ M^{-1}\,s^{-1}$ (*38*) was used in the model.

2-propanone generated versus the einsteins of light absorbed was linear, with a slope of 0.91 ± 0.12 mol einstein^{-1}. Using this value in eq 7, Φ_{RH} was calculated to be 1.05 ± 0.14. This compares well to literature values (e.g., 0.98 ± 0.03 at pH = 7, $T = 298$ K, $\lambda = 308$ nm (*30*); 0.98 ± 0.07 at 298 K, $\lambda = 254$ nm (*31*); and 0.49 ± 0.065 mol H_2O_2 degraded per einstein absorbed at 253.7 nm, 298 K (*32*)).

The Validated Reaction Mechanism. The set of main reactions used in the kinetic model is presented in Table 1. Reactions 3–5 can be collapsed into one reaction, since the short lifetime of the oxalyl radical should preclude it from participation in other reactions, and its decarboxylation product, $CO_2^{\bullet -}$, is not involved in any other significant reactions:

$$Fe^{III}(C_2O_4)_3^{3-} \xrightarrow{h\nu} Fe^{2+} + CO_2 + 2.5C_2O_4^{2-}\ (\Phi_{Fe(II)}N_a/V) \quad (8)$$

There are no other significant photochemical reactions (e.g., H_2O_2 photolysis) because the reactant concentrations and the molar extinction coefficients of the reactants are such that ferrioxalate is the predominant absorber. No effect on $\Phi_{Fe(II)}$ (300 nm) was observed for the different ferrioxalate concentrations used in this study (where Fe(III) was coordinated with either two or three ligands) so the di- and trioxalato complexes were considered kinetically equivalent. The Fe(II) produced in reaction 8 then generates ${}^\bullet OH$ via the Fenton reaction (reaction 6).

The hydroxyl radical may react with a variety of species, but under conditions of excess 2-propanol, it reacts primarily with 2-propanol. The predominant oxidation route of 2-propanol (HROH) involves α-hydrogen abstraction generating the 1-hydroxy-1-methylethyl radical (${}^\bullet ROH$):

$${}^\bullet OH + HROH \xrightarrow{k_9} {}^\bullet ROH + H_2O \quad (9)$$

At lower concentrations of 2-propanol, the following scavenging reactions become competitive:

$${}^\bullet OH + H_2O_2 \xrightarrow{k_{10}} H_2O + HO_2^\bullet \quad (10)$$

$${}^\bullet OH + HC_2O_4^- \xrightarrow{k_{11}} H_2O + C_2O_4^{\bullet -} \quad (11)$$

When this occurs, Φ_{RH} cannot serve as an indirect measure of Φ_{OH}. The monobasic form of oxalate $HC_2O_4^-$ is the

$${}^\bullet OH + SO_4^{2-} + H^+ \xrightarrow{k_{12}} H_2O + SO_4^{\bullet -} \quad (12)$$

dominant form of free oxalate at the pH used in the experiments. However, the symbol $HC_2O_4^-$ in reaction 11 is used to represent all of the oxalate in solution, both free (mono- and dibasic) and coordinated, since it is assumed that ${}^\bullet OH$ will still attack oxalate when it is coordinated with Fe(III). Reaction 12 involves both the mono- and dibasic sulfate anions, since the ratio of SO_4^{2-} to HSO_4^- is 1.9 at pH 2.2. The sulfate anions in the solution matrix are from the original Fe(III) stock solution.

The reducing radical ${}^\bullet ROH$ may be oxidized to 2-propanone (RO) by one of two competing routes (*33*):

$${}^\bullet ROH + Fe^{III}(C_2O_4)_3^{3-} \xrightarrow{k_{13}} RO + Fe^{2+} + 2C_2O_4^{2-} + HC_2O_4^- \quad (13)$$

$${}^\bullet ROH + O_2 \xrightarrow{k_{14}} RO + HO_2^\bullet \quad (14)$$

Reaction 13 is a chain-propagating step because it potentially leads to enhanced ${}^\bullet OH$ production, via reaction 6, without the requirement of further light absorption. Reactions 14 and 10 produce the hydroperoxyl radical $HO_2^\bullet$ (*34*) which may oxidize Fe(II) and generate H_2O_2. The protonated form of $HO_2^\bullet$ is dominant at pH 2.2, with <0.4% as $O_2^{\bullet -}$. Reaction 15 is competitive when the concentration of H_2O_2 is sufficiently low:

$$Fe^{2+} + HO_2^\bullet + H^+ + 3C_2O_4^{2-} \xrightarrow{k_{15}} Fe^{III}(C_2O_4)_3^{3-} + H_2O_2 \quad (15)$$

Here, the reaction rate depends on k_{15}, the second-order rate constant and the concentrations of Fe^{2+} and $HO_2^\bullet$. Fe^{2+} represents any Fe(II) species, including $[Fe^{II}C_2O_4]^0$, that can react with $HO_2^\bullet$, although the rate constant is reported only for uncomplexed Fe(II).

The hydroperoxyl radical may also dismutate to H_2O_2 and oxygen

$$HO_2^\bullet + HO_2^\bullet \xrightarrow{k_{16}} H_2O_2 + O_2 \quad (16)$$

or it may react with ferrioxalate

$$HO_2^{\bullet} + Fe^{III}(C_2O_4)_3^{3-} \xrightarrow{k_{17}} Fe^{2+} + H^+ + O_2 + 3C_2O_4^{2-} \quad (17)$$

The rate constant for this reaction is not known, although the reaction is reported to be very slow (*22*).

Kinetic Modeling. A kinetic simulation program was written in Turbo Pascal 5.0 to calculate Φ_{RH} using a reiterative process over time (for a similar treatment, see ref *35*). Reactions 6 and 8−17 (see Table 1) were used to write differential equations expressing the rate of change of the concentration of each species. For example, the change in oxygen concentration over a very small time interval δt based on the proposed reaction mechanism is:

$$\delta[O_2] = (-k_{12}[^{\bullet}ROH][O_2] + k_{14}[HO_2^{\bullet}][HO_2^{\bullet}])\delta t \quad (18a)$$

This allows the determination of $[O_2]$ at time $t + \delta t$:

$$[O_2]_{t+\delta t} = [O_2]_t + \delta[O_2] \quad (18b)$$

Differential equations were used as above for all species except $^{\bullet}OH$ and $^{\bullet}ROH$, for which steady-state expressions were derived. Thus the initial concentrations of reactants at time $t = 0$ s were used to determine the remaining reactant and the intermediate concentrations after the time interval δt, at time $t + \delta t$, where δt was 0.1 μs. This process (approximation by finite differences) was repeated up to a final time $t_f = 10$ s (a typical exposure time for experiments was ~30 s). The quantum yields, Φ_{RH}, at $t_f = 10$ s, calculated using the molar concentration of 2-propanol oxidized and the number of einsteins of light absorbed per liter, were generated for a variety of initial reaction conditions corresponding to those experimentally used. The four theoretical data sets thus generated were compared simultaneously to the four experimental data sets (each data set varied by one reactant concentration, either that of 2-propanol, ferrioxalate, H_2O_2, or oxygen).

In general, there was reasonable agreement between the theoretical and the experimental Φ_{RH} values (Figures 2−5), suggesting that the proposed reaction mechanism adequately describes the UV−vis/ferrioxalate/H_2O_2 system. The Φ_{RH} values were often significantly greater than unity, with maximum values above 6 (Figure 3).

All experimental Φ_{RH} values are plotted with 95% confidence intervals. Random exposure of the samples to stray light, a parameter that was extremely difficult to control, and gas chromatographic analyses of the aqueous samples were the largest contributors to error.

Literature values were found for most of the rate constants and used in the model. However, several rate constants (k_{11}, k_{13}, k_{17}) and an equilibrium constant (K_{FeOx} used to calculate k_6) were either not found in the literature or not well established. All except k_{17} were used as "adjustable" parameters, varied to achieve a better fit of the theoretical quantum yields to all four sets of the experimental data simultaneously.

The rate constant k_{17} for the reaction between ferrioxalate and the hydroperoxyl radical is an apparent rate constant since a very small fraction (0.32%) of $HO_2^{\bullet}$ is deprotonated $O_2^{\bullet-}$. While $HO_2^{\bullet}$, the dominant species, is known to react with free iron(III), it does so at a much slower rate than with iron(II) (*36*, *38*). Furthermore, Sedlak and Hoigné reported that these radicals are essentially unreactive with ferrioxalate, but that the rate constants for $HO_2^{\bullet}/O_2^{\bullet-}$ are below 1.2×10^5 and 1×10^6 M^{-1} s^{-1}, respectively (*22*). Since these are only upper limits, the rate constants may be much lower. The parameter k_{17} was set to 3.5×10^3 M^{-1} s^{-1} and the remaining adjustable parameters varied, keeping k_{17} constant.

The model was most sensitive to k_{13}, for the reaction between $^{\bullet}ROH$ and ferrioxalate, which had a global effect on the kinetic simulation, that is, it had a strong effect on the output under all initial reaction conditions. For example, a 90% increase in k_{13} from 4.0×10^8 to 7.5×10^8 resulted in a 40% increase in Φ_{RH}. Therefore, k_{13} was the first parameter varied to fit the theoretical quantum yields simultaneously

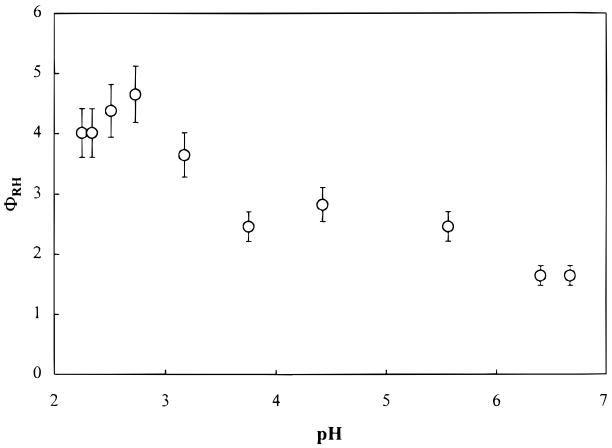

FIGURE 1. Effect of initial pH on Φ_{RH} (with 95% confidence intervals). Conditions: $\lambda = 300$ nm, 0.27 mM O_2, 3.79 mM $Fe^{III}(C_2O_4)_3^{3-}$, 10.2 mM H_2O_2, 28.3 mM 2-propanol.

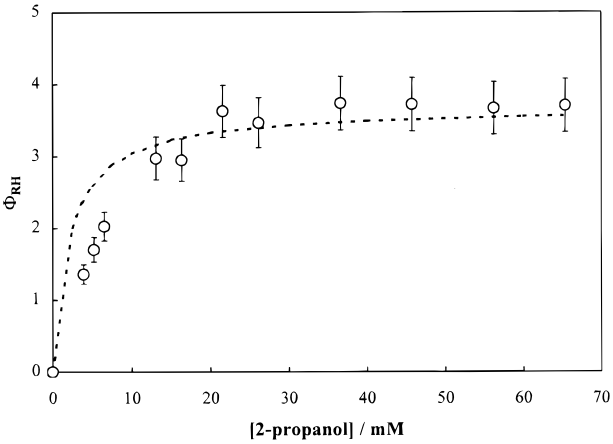

FIGURE 2. The dependence of Φ_{RH} on initial 2-propanol concentration: (○) mean experimental Φ_{RH} with 95% confidence intervals; (- - -) theoretical Φ_{RH}. Conditions: $\lambda = 300$ nm, pH 2.2, 0.27 mM O_2, 4.0 mM $Fe^{III}(C_2O_4)_3^{3-}$, 10.0 mM H_2O_2, $N_a/V = 2.34 \times 10^{-6}$ einstein L^{-1} s^{-1}.

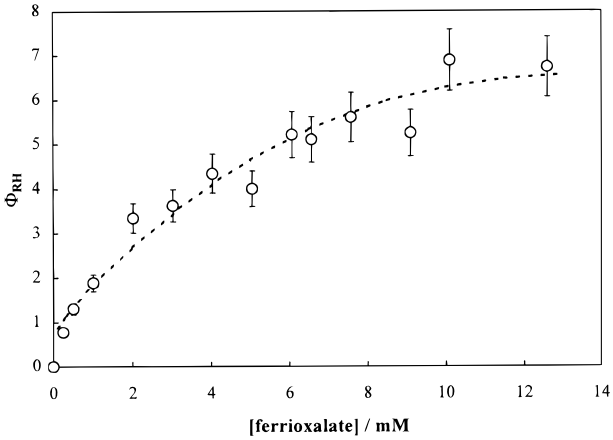

FIGURE 3. Effect of $Fe^{III}(C_2O_4)_3^{3-}$ concentration on Φ_{RH}: (○) mean experimental Φ_{RH} with 95% confidence intervals; (- - -) theoretical Φ_{RH}. Conditions: $\lambda = 300$ nm, pH 2.7 ± 0.1, 0.27 mM O_2, 11.0 mM H_2O_2, 30.0 mM 2-propanol, $N_a/V = 2.94 \times 10^{-6}$ einstein L^{-1} s^{-1}.

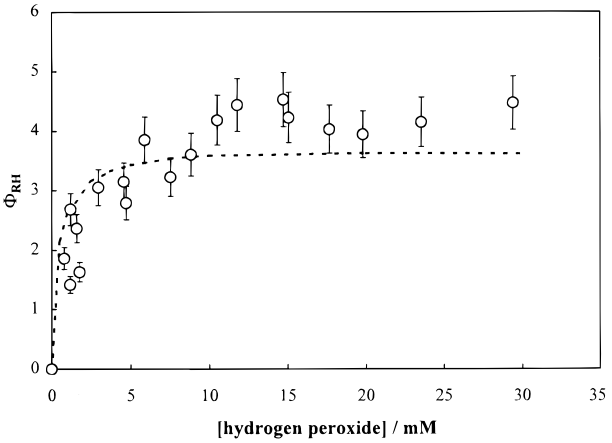

FIGURE 4. Effect of initial H_2O_2 concentration on Φ_{RH}: (○) mean experimental Φ_{RH} with 95% confidence intervals; (- - -) theoretical Φ_{RH}. Conditions: $\lambda = 300$ nm, pH = 2.2, 0.27 mM O_2, 3.5 mM $Fe^{III}(C_2O_4)_3^{3-}$, 26.3 mM 2-propanol, $N_a/V = 1.31 \times 10^{-6}$ einstein L^{-1} s^{-1}.

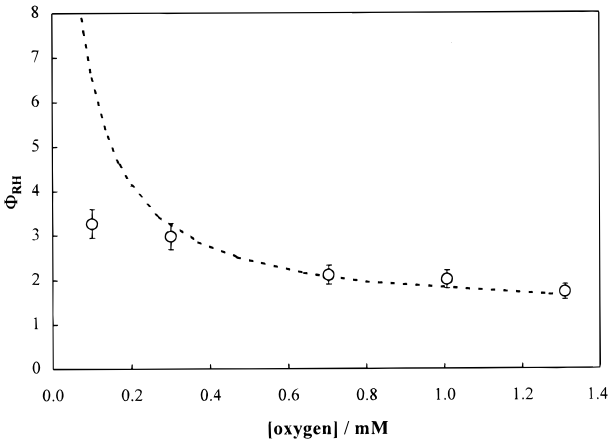

FIGURE 5. Effect of initial O_2 concentration on Φ_{RH}: (○) mean experimental Φ_{RH} with 95% confidence intervals; (- - -) theoretical Φ_{RH}. Conditions: $\lambda = 300$ nm, pH 2.2, 3.3 mM $Fe^{III}(C_2O_4)_3^{3-}$, 10.2 mM H_2O_2, 24.7 mM 2-propanol, $N_a/V = 1.43 \times 10^{-6}$ einstein L^{-1} s^{-1}.

to the four experimental data sets used in the comparison. The optimal value was 7.5×10^8 M^{-1} s^{-1}, which is consistent with literature values for uncomplexed iron(III) (*37*) and with reports that carbon-centered radicals are expected to react rapidly with iron(III)−carboxylate species (*23*).

The Fenton reaction represents the sum of Fe^{2+} (the predominant species) and $[Fe^{II}C_2O_4]^0$ reacting with H_2O_2 and so k_6 is an apparent rate constant, dependent on the relative mole fractions of the Fe(II) species and their respective rate constants for reaction with H_2O_2 (*22*). Since the rate constants for reaction of each with H_2O_2 differ by several orders of magnitude (63 M^{-1} s^{-1} at room temperature (*39*) and $(3.1 \pm 0.6) \times 10^4$ M^{-1} s^{-1}, respectively (*22*)), even a small fraction of $[Fe^{II}C_2O_4]^0$ can substantially increase the apparent rate constant, k_6. The equilibrium constant K_{FeOx} for $[Fe^{II}C_2O_4]^0$, used to calculate the mole fractions of Fe^{2+} and $[Fe^{II}C_2O_4]^0$ for each set of initial reaction conditions, was treated as an adjustable parameter, since it is reported that the magnitude of K_{FeOx} is not well established (*22*). K_{FeOx} was set to 5.9×10^3 M^{-1} and used in the calculation of k_6 for each set of initial reaction conditions. The model was most sensitive to K_{FeOx} at lower concentrations of H_2O_2. For example, decreasing the value 5.9×10^3 by 80% resulted in a 30% decrease of Φ_{RH} in 10 mM H_2O_2.

The parameter k_{11}, for the reaction between •OH and $HC_2O_4^-$ (free or coordinated) was used as an adjustable parameter. It had an effect on the kinetic simulation under conditions where 2-propanol was not completely scavenging •OH, i.e., at low 2-propanol concentrations or high ferrioxalate concentrations. A 90% change in the value k_{11} from 4.7×10^7 to 9.0×10^7 M^{-1} s^{-1} decreased Φ_{RH} by 10% when the concentration of ferrioxalate was 8.5 mM. While the literature value for k_{11} involving monobasic oxalate (4.7×10^7 M^{-1} s^{-1} (*2*)) gave reasonable results, an improved fit of the theoretical to the experimental data was obtained using 9.0×10^7 M^{-1} s^{-1}.

The literature value of the rate constant k_{12} for the reaction between •OH and the monobasic sulfate anion HSO_4^- (*2*) was used in the kinetic model since a rate constant for the reaction involving SO_4^{2-} was not found.

The rate constant k_{15} has been reported for the reaction between uncomplexed Fe(II) and the hydroperoxyl radical, but we are not aware of any literature reports of Fe(II) oxalate reacting with HO_2•. Therefore, the model contains the assumption that all the Fe(II) is uncomplexed with respect to reaction 15 only. This assumption and the literature value for the reaction between uncomplexed Fe(II) and the hydroperoxyl radical gave agreeable results.

Dependence of Φ_{RH} on Various Factors. To demonstrate clearly the role that each reaction parameter plays in the UV−vis/ferrioxalate/H_2O_2 system, the initial pH and each of the principal reactant species (HROH, $Fe^{III}(C_2O_4)_3^{3-}$, H_2O_2, and O_2) are examined, individually, as to how they influence Φ_{RH}.

pH. The pH used for most experiments was 2.2, at which point the Φ_{RH} values are relatively high (Figure 1). They remain higher than unity, even above pH 6. A maximum value of $\Phi_{RH} = 4.6 \pm 0.5$ (95% confidence) was observed at pH 2.7, although Φ_{RH} is relatively independent of the pH between 2.2 and 2.7, within experimental error.

2-Propanol Concentration. Most experiments were conducted using relatively high concentrations of 2-propanol (∼27 mM), such that it was the sole scavenger of •OH. The minimum concentration of 2-propanol (for the given experimental conditions) required to meet this condition is illustrated by a plot (Figure 2) of Φ_{RH} against the initial scavenger concentration. In the region of curvature, 2-propanol competes with other species, predominantly H_2O_2, oxalate, and sulfate anions (reactions 10, 11, and 12), for •OH. Eventually, the Φ_{RH} value reaches a plateau (22 mM 2-propanol, $\Phi_{RH} = 3.6 \pm 0.4$), at which point 2-propanol reacts with virtually all of the hydroxyl radicals generated, and Φ_{RH} becomes independent of 2-propanol concentration. In this region Φ_{RH} is equal to Φ_{OH}.

Additional •OH scavengers include Fe(II), the hydroperoxyl radical (*36*), 2-propanone, and •OH itself, all of which were in solution at very low concentrations. None of these reactions had an influence on the theoretical quantum yield when added to the kinetic model, even with 3.0 mM 2-propanol, where an effect would be more evident. Nor was a cumulative effect observed using all of the scavengers simultaneously in the model.

Ferrioxalate Concentration. Ferrioxalate has a high molar absorption coefficient such that, at the concentrations used in this study and over the range 200−400 nm, all incident light is absorbed. The molar absorption coefficient then decreases to zero at ∼550 nm. The quantum yield of Fe(II) generation from ferrioxalate photolysis, $\Phi_{Fe(II)}$, remains high from 200 to 500 nm (e.g., ∼0.90 at 502 nm (*7*)). These two factors help to make the UV−vis/ferrioxalate/H_2O_2 system an extremely efficient producer of •OH (via reaction 6) relative to other AOTs.

It was found that Φ_{RH} values are independent of the incident light flux over the range $(0.16-1.4) \times 10^{-8}$ einstein s^{-1}. Also, Φ_{RH} values were found to be independent of the wavelength of irradiation between 240 and 425 nm (Table 2).

TABLE 2. Φ_{RH} Values (± One Standard Deviation) over the Wavelength Range 240−425 nm[a]

wavelength/nm	Φ_{RH}
240	3.0 ± 0.16
269	2.7 ± 0.14
300	3.0 ± 0.15
360	2.9 ± 0.15
425	2.5 ± 0.3

[a] Initial conditions: 3.8 mM $Fe^{III}(C_2O_4)_3^{3-}$, 10 mM H_2O_2, 27 mM 2-propanol, pH 2.2.

We therefore expect that high efficiencies will be obtained when using solar radiation.

The trend in Φ_{RH} values as a function of wavelength should mirror that of $\Phi_{Fe(II)}$ values, under the same reaction conditions. The literature values of $\Phi_{Fe(II)}$ vary by about 10% over the wavelength range studied (*7*). However, the experimental results reported here are not inconsistent because the errors are too large to allow discrimination of a similar variation in the experimental Φ_{RH} values.

Ferrioxalate is the primary light absorber, but it is also involved in an important dark reaction. It competes with oxygen for the 1-hydroxy-1-methylethyl radical (a strong reducing agent) in reaction 13. This reaction increases the quantum yield because it produces more Fe(II) without requiring light energy.

Figure 3 plots Φ_{RH} against the ferrioxalate concentration in solutions with a pH of 2.7 ± 0.1. The three other data sets were obtained using pH 2.2. Since Φ_{RH} was relatively independent of pH from pH 2.2 to 2.7, the ferrioxalate results were included in the experimental data sets used to optimize the adjustable parameters in the kinetic model. The theoretical values of Φ_{RH} compare very well to the experimental data points.

The attenuation of the rate of increase in the experimental Φ_{RH} at high ferrioxalate concentrations is explained by an increase in $^{\bullet}OH$ scavenging by oxalate and sulfate (reactions 11 and 12). The concentrations of both scavengers increased with the initial concentration of Fe(III) since the total initial concentration of oxalate was 3.2 times that of Fe(III) and the initial concentration of sulfate 5.5 times that of Fe(III). The immediate effect of reactions 11 and 12 is the prevention of 2-propanol oxidation by $^{\bullet}OH$ attack. However, neither reaction is necessarily an end to chain propagation. The oxalyl radical produces $CO_2^{\bullet-}$ which can reduce ferrioxalate (reaction 5), and the sulfate radical is an oxidizing radical capable of 2-propanol attack.

Hydrogen Peroxide Concentration. Φ_{RH} is independent of H_2O_2 concentrations above 10.5 mM where $\Phi_{RH} = 4.2 \pm 0.4$ (Figure 4). Above this level, no other species can effectively compete with H_2O_2 for Fe(II) so all Fe(II) reacts via reaction 6 to produce $^{\bullet}OH$. Eventually, at sufficiently high H_2O_2 concentrations, H_2O_2 will also scavenge $^{\bullet}OH$ (reaction 10) and Φ_{RH} should decrease. While reaction between H_2O_2 and the 1-hydroxy-1-methylethyl radical is possible the relatively

$$H_2O_2 + {}^{\bullet}ROH \xrightarrow{k_{19}} RO + H_2O + {}^{\bullet}OH \qquad (19)$$

low rate constant ($4.77 \times 10^5\ M^{-1}\ s^{-1}$ (*37*)) renders this reaction unable to compete with reactions 13 and 14 under any of the reaction conditions used to obtain the experimental data.

Below 10 mM H_2O_2, the Φ_{RH} dependence on H_2O_2 concentration indicates that there are other competitive reactions for Fe(II). To ensure that this was not an effect of precipitating the iron before all dark reactions were complete, 10 M NaOH was added to solutions at either 3−5 s or 5 min after irradiation. An effect was not observed, indicating that no dark reactions (e.g., the Fenton reaction) were interrupted when the solutions were deactivated immediately after irradiation. Also, there was no detectable change in the concentration of H_2O_2 after irradiation, so this was not a problem of H_2O_2 depletion.

Oxygen is known to react with Fe(II), but work conducted in this investigation and others, such as that done by Zuo and Hoigné (*21*) who investigated iron cycling in atmospheric waters, suggests that the oxidation of photogenerated Fe(II) by oxygen (in the presence of oxalate) is negligible with respect to other iron-cycling reactions. Also, the kinetic model indicates that the $^{\bullet}OH$ concentration remains too low for it to compete for Fe(II). Rather, Fe(II) oxidation is thought to occur, in acidic media, by reaction with the hydroperoxyl radical $HO_2^{\bullet}$ (reaction 15). We included this in the reaction mechanism, assuming that reaction 15 could be a dominant, alternative oxidation route for Fe(II). The simulation program indicates that the concentration of $HO_2^{\bullet}$ can build to relatively high levels (10^{-7} M), despite its removal by reactions 16 and 17. This would allow it to compete effectively for Fe(II) when the H_2O_2 concentration is low.

Reactions 15 and 16 produce H_2O_2, but at levels that are negligible relative to the initial H_2O_2 concentrations used in these experiments.

Hydrogen peroxide is known to react with the carbon dioxide radical anion, produced by reaction 4, to generate $^{\bullet}OH$ ($k = 7.3 \times 10^5\ M^{-1}\ s^{-1}$ (*40*)). However, modeling results suggest that this is insignificant.

Oxygen Concentration. Oxygen prevents the 1-hydroxy-1-methylethyl radical from generating Fe(II) via reaction 13. However, there is still the possibility for Fe(II) production since the hydroperoxyl radical may reduce ferrioxalate (reaction 17). As expected, Φ_{RH} decreases (Figure 5) with increasing oxygen concentration. This behavior is best understood in terms of a competition between ferrioxalate and oxygen for the $^{\bullet}ROH$ radical (reactions 13 and 14). If $^{\bullet}ROH$ reacts with ferrioxalate, more Fe(II) is generated. Thus, under low oxygen concentrations, Φ_{RH} increases.

The data point shown for 0.1 mM oxygen is lower than the calculated value of Φ_{RH}. While this may be an experimental artifact, the incorporation of only two pathways for the oxidation of $^{\bullet}ROH$ (reactions 13 and 14) may oversimplify the mechanism. Other chain-terminating reactions may exist that limit the maximum Φ_{RH} value achievable at low oxygen concentrations.

We considered the possibility of reaction between oxygen and the carbon dioxide radical anion, produced in reaction 4:

$$CO_2^{\bullet-} + O_2 \xrightarrow{k_{20}} O_2^{\bullet-} + CO_2 \qquad (20)$$

$$O_2^{\bullet-} + H^+ \rightleftharpoons HO_2^{\bullet} \qquad (21)$$

Here, $k_{20} = 2.4 \times 10^9\ M^{-1}\ s^{-1}$ (*22*), and the pK_a for the deprotonation of $HO_2^{\bullet}$ (the reverse of reaction 21) is 4.8 (*36*).

Two observations led to the exclusion of these reactions from the proposed reaction mechanism. First, there was no measurable effect on the rate of Fe(II) generation from the photolysis of 1 mM or 10 mM ferrioxalate (in the absence of 2-propanol and H_2O_2) containing either 0.08 mM or 0.81 mM oxygen. Such an effect would be due to carbon dioxide radical anion scavenging by oxygen, leading to a decreased rate of Fe(II) generation via reaction 5.

Second, the exclusion of reactions 20 and 21 from the reaction mechanism had a negligible effect on the theoretical Φ_{RH} values. This is consistent with the experimental observation that oxygen does not compete effectively with ferrioxalate for $CO_2^{\bullet-}$ under these experimental conditions. The carbon dioxide radical anion is a strong reducing agent, and many literature values for rate constants involving $CO_2^{\bullet-}$ are

TABLE 3. Φ_{RH} Values (with 95% Confidence Intervals) for Different Alcohols Using 300-nm Light

scavenger (RH)	[RH], mM	[H_2O_2], mM	[$Fe^{III}(C_2O_4)_3^{3-}$], mM	$\Phi_{Product}$	Φ_{OH}
2-propanol	22−65	10.23	3.29	3.16 ± 0.08	3.65 ± 0.09
methanol	101	12.96	3.29	3.26 ± 1.2	3.26 ± 1.2
tert-butanol	80−400	12.96	3.29	0.535 ± 0.036	2.23 ± 0.15

near the diffusion-limited rate (*40*). This should also be the case for the reaction between ferrioxalate and $CO_2^{\bullet-}$, such that reaction 20 is important only at very low, catalytic ferrioxalate concentrations (*25*).

The presence of oxygen, while it does prevent $^{\bullet}$ROH from cycling Fe(III) to Fe(II), does not seriously limit the efficiency of this system ($\Phi_{RH} = 3.0$ in 0.3 mM O_2; $\Phi_{RH} = 1.7$ in 1.3 mM O_2), especially in light of the quantum efficiencies that have been attained by other AOTs. Furthermore, applications of this system to water treatment would see longer treatment times for HROH and the consumption of oxygen via reaction 14.

The value Φ_{RH} was equivalent to Φ_{OH} under all experimental conditions except at low 2-propanol concentrations and high ferrioxalate concentrations. Relatively high Φ_{RH} values were obtained over a wide range of initial reactant conditions, demonstrating that the UV−vis/ferrioxalate/H_2O_2 system is very efficient as a photochemical method for $^{\bullet}$OH production when the target pollutant(s) generates reducing radicals such as the α-hydroxyalkyl radical produced from 2-propanol. These reducing radicals increase dark cycling of Fe(III) to Fe(II).

However, iron cycling of this type is only possible when the organo radical is easily oxidized. Other organic substrates may produce radicals that resist oxidation (*33*, *41*, *42*). Such radicals could have lifetimes sufficiently long to allow dimerization, or they could compete with H_2O_2 for Fe(II), thereby decreasing the chain length of the system and reforming the parent organic molecule RH:

$$R^{\bullet} + Fe^{2+} + H^{+} \rightarrow Fe^{3+} + RH \qquad (22)$$

Under the reaction conditions used in this study, however, reaction 22 is negligible, even for diffusion-limited rate constants since the low concentration of Fe(II) does not permit it to compete with oxygen for the organo radical. Therefore, the maximum value of Φ_{RH} possible in the absence of reducing radicals is equal to $\Phi_{Fe(II)}$, the quantum yield of Fe(II) generation during the photoreduction of ferrioxalate.

Two other alcohols were used as model substrates in the UV−vis/ferrioxalate/H_2O_2 system: methanol and *tert*-butyl alcohol. Sufficient concentrations were used to ensure complete $^{\bullet}$OH scavenging by the alcohol so that the quantum yield of substrate degradation, Φ_{RH}, was equivalent to Φ_{OH}. The Φ_{RH} value obtained using methanol, which is quantitatively oxidized to formaldehyde, was very similar to that obtained using 2-propanol (Table 3). This is consistent with the behavior of the principal oxidation intermediate of methanol, the hydroxymethyl radical, which has similar reducing properties to the α-hydroxyalkyl radical formed from 2-propanol. Thus, dark cycling of Fe(III) to Fe(II) by the organo radical led to an increase in the quantum yield.

The oxidation of *tert*-butyl alcohol, on the other hand, leads predominantly to the formation of a β-hydrogen abstracted radical, which is unreactive with ferrioxalate. The absence, then, of dark Fe(III) to Fe(II) cycling by the organo radical should lead to reduced values of Φ_{RH}. The oxidation of *tert*-butyl alcohol involves the formation of a number of stable products, one of which is 2-propanone (*43*). The yield of 2-propanone from *tert*-butyl alcohol was found to be 0.24 ± 0.06 by measuring the formation of 2-propanone after a known number of hydroxyl radicals were generated by photolyzing H_2O_2 (no ferrioxalate present) at 254 nm using a calibrated light source. This value (analogous to the factor 0.867 used in eq 7) allowed the determination of the amount of *tert*-butyl alcohol that was oxidized in the UV−vis/ferrioxalate/H_2O_2 system. The value of Φ_{RH} in Table 3 is lower than that found using either 2-propanol or methanol and can be attributed in part to the absence of iron cycling by the β-radical. However, the magnitude of Φ_{RH} is greater than $\Phi_{Fe(II)}$, the maximum value expected in the absence of any dark iron cycling by an organo radical. This suggests that iron cycling is still occurring, albeit at a reduced rate. Inspection of the oxidation pathways suggested for the β-radical (*43*) reveals that one oxidation route involves the formation of the 1-hydroxy-1-methylethyl radical, the same radical generated by α-hydrogen abstraction from 2-propanol. Since this radical is strongly reducing, it may react with ferrioxalate to form Fe(II) (reaction 13). These results highlight the importance of dark Fe(III) to Fe(II) cycling by organo radicals to the efficiency of the UV−vis/ferrioxalate H_2O_2 system.

Acknowledgments

This project has been supported in part by a Natural Sciences and Engineering Research Council of Canada Collaborative Research and Development Grant with Calgon Carbon Corporation, Markham, Ontario, Canada. Appreciation is extended to Dr. Stephen Cater of Calgon Carbon Corporation, Dr. Ali Safarzadeh-Amiri, and Dr. Mihaela Stefan for critical reviews of the manuscript.

Literature Cited

(1) Fenton, H. J. H. *J. Chem. Soc., Trans.* **1894**, *65*, 899−910.
(2) Buxton, G. V.; Greenstock, C. L.; Helman, W. P.; Ross, A. P. *J. Phys. Chem. Ref. Data* **1988**, *17*, 513−886.
(3) Faust, B. C.; Hoigné, J. *Atmos. Environ.* **1990**, *24A*, 79−89.
(4) Graedel, T. E.; Mandich, M. L.; Weschler, C. J. *J. Geophys. Res.* **1986**, *91*, 5205−5221.
(5) Baxendale, J. H.; Magee, J. *Trans. Faraday Soc.* **1955**, *51*, 205−213.
(6) Benkelberg, H.-J.; Warneck, P. *J. Phys. Chem.* **1995**, *99*, 5214−5221.
(7) Murov, S. L.; Carmichael, I.; Hug, G. L. *Handbook of Photochemistry*, 2nd ed.; Marcel Dekker: New York, 1993; pp 299−305.
(8) Hatchard, C. G.; Parker, C. A. *Proc. R. Soc. London, Ser. A* **1956**, *235*, 518−536.
(9) Balzani, V.; Carassiti, V. *Photochemistry of Coordination Compounds;* Academic Press: London and New York, 1970; pp 145−191.
(10) Mulazzani, Q. G.; D'Angelantonio, M.; Venturi, M.; Hoffman, M. Z.; Rodgers, M. A. *J. Phys. Chem.* **1986**, *90*, 5347−5352.
(11) Cooper, G. D.; DeGraff, B. A. *J. Phys. Chem.* **1971**, *75*, 2897−2902.
(12) Cooper, G. D.; DeGraff, B. A. *J. Phys. Chem.* **1972**, *76*, 2618−2625.
(13) Zepp, R. G.; Faust, B. C.; Hoigné, J. *Environ. Sci. Technol.* **1992**, *26*, 313−319.
(14) Safarzadeh-Amiri, A.; Bolton, J. R.; Cater, S. R. *The Role of Iron in Advanced Oxidation Processes*; The First International Conference on Advanced Oxidation Technologies for Water and Air Remediation, London, Ontario, Canada, London Convention Centre, June 25−30, 1994.
(15) Safarzadeh-Amiri, A. Photocatalytic Method for Treatment of Contaminated Water. U.S. Patent 5266214, 1993.
(16) Safarzadeh-Amiri, A.; Bolton, J. R.; Cater, S. R. *Water Res.* **1997**, *31*, 787−798.

(17) Sun, Y.; Pignatello, J. J. *J. Agric. Food Chem*. **1993**, *41*, 308−312.
(18) Tolman, C. A.; Tumas, W.; Lee, S. Y. L.; Campos, D. In *The Activation of Dioxygen and Homogeneous Catalytic Oxidation;* Barton, D. H. R., Ed.; Plenum Press: New York, 1993; pp 57−70.
(19) Safarzadeh-Amiri, A.; Bolton, J. R.; Cater, S. R. *Sol. Energy* **1996**, *56*, 439−443.
(20) Safarzadeh-Amiri, A.; Bolton, J. R.; Cater, S. R. *J. Adv. Oxid. Technol.* **1996**, *1*, 18−26.
(21) Zuo, Y.; Hoigné, J. *Environ. Sci. Technol.* **1992**, *26*, 1014−1022.
(22) Sedlak, D. L.; Hoigné, J. *Atmos. Environ*. **1993**, *27A*, 2173−2185.
(23) Faust, B. C.; Zepp, R. G. *Environ. Sci. Technol.* **1993**, *27*, 2517−2522.
(24) Voelker, B. M.; Morel, F. M. M.; Sulzberger, B. *Environ. Sci. Technol.* **1997**, *31*, 1004−1011.
(25) Huston, P. L.; Pignatello, J. J. *Environ. Sci. Technol.* **1996**, *30*, 3457−3463.
(26) Kawaguchi, H. *Chemosphere* **1993**, *27*, 577−584.
(27) Asmus, K.-D.; Möckel, H.; Henglein, A. *J. Phys. Chem*. **1973**, *77*, 1218−1221.
(28) Klassen, N. V.; Marchington, D.; McGowan, H. C. E. *Anal. Chem*. **1994**, *66*, 2921−2925.
(29) Wells, C. F. *Tetrahedron* **1966**, *22*, 2685−2693.
(30) Zellner, R.; Exner, M.; Herrmann, H. *J. Atmos. Chem*. **1990**, *10*, 411−425.
(31) Kryschi, R.; Gürtler, K. R.; Perkampus, H.-H. *Vom Wasser* **1988**, *70*, 197−207.
(32) Weeks, J. L.; Matheson, M. S. *J. Am. Chem. Soc.* **1956**, *78*, 1273−1279.
(33) Walling, C. *Acc. Chem. Res.* **1975**, *8*, 125−131.
(34) Bothe, E.; Schuchmann, M. N.; Schulte-Frohlinde, D.; von Sonntag, C. *Photochem. Photobiol.* **1978**, *28*, 639−644.
(35) Stefan, M. I.; Hoy, A. R.; Bolton, J. R. *Environ. Sci. Technol.* **1996**, *30*, 2382−2390.
(36) Bielski, B. H. J.; Cabelli, D. E.; Arudi, R. L.; Ross, A. B. *J. Phys. Chem. Ref. Data* **1985**, *14*, 1041−1100.
(37) Neta, P.; Grodkowski, J.; Ross, A. B. *J. Phys. Chem. Ref. Data* **1996**, *25*, 709−1050.
(38) Rush, J. D.; Bielski, B. H. J. *J. Phys. Chem*. **1985**, *89*, 5062−5066.
(39) Hardwick, T. J. *Can. J. Chem*. **1957**, *35*, 428−436.
(40) Neta, P.; Huie, R. E.; Ross, A. B. *J. Phys. Chem. Ref. Data* **1988**, *17*, 1027−1284.
(41) Merz, J. H.; Waters, W. A. *J. Chem. Soc.* **1949**, *Part 4*, 2427−2433.
(42) Merz, J. H.; Waters, W. A. *J. Chem. Soc.* **1949**, *(Suppl. 1 & 2)*, S15−S25.
(43) Schuchmann, M. N.; von Sonntag, C. *J. Phys. Chem*. **1979**, *83*, 780−784.

Received for review October 1, 1998. Revised manuscript received April 26, 1999. Accepted May 22, 1999.

ES9810134